Gene 470 (2011) 37–45

Contents lists available at ScienceDirect

Gene

journal homepage: www.elsevier.com/locate/gene

Characterisation and comparative analysis of MHC-DPA1 exon 2 in the owl monkey (*Aotus nancymaae*)

Carlos F. Suárez M. [a,b], Manuel A. Patarroyo [a,b], Manuel E. Patarroyo [a,c,*]

[a] *Fundación Instituto de Inmunología de Colombia (FIDIC), Carrera 50 No. 26-20, Bogotá, Colombia*
[b] *Universidad del Rosario, Calle 63D No. 24-31, Bogotá, Colombia*
[c] *Universidad Nacional de Colombia, Carrera 45 No. 26-85 Bogotá, Colombia*

ARTICLE INFO

Article history:
Accepted 17 September 2010
Available online 25 September 2010

Received by Leonardo Marino-Ramirez

Keywords:
Animal model
MHC class II molecule
Molecular evolution
New world monkeys
Platyrrhini

ABSTRACT

The *Aotus nancymaae* (owl monkey) is an important animal model in biomedical research, particularly for the preclinical evaluation of vaccine candidates against *Plasmodium falciparum* and *Plasmodium vivax*, which require a precisely typed major histocompatibility complex. The exon 2 from *A. nancymaae* MHC-DPA1 gene was characterised in order to infer its allelic diversity and evolutionary history. Aona-DPA1 shows no polymorphism and is related to other primate DPA alleles (including Catarrhini and Platyrrhini), constituting an ancient trans-specific and strongly supported lineage with different variability and selective patterns when compared to other primate–MHC-DPA1 lineages. *A. nancymaae* monkeys have thus a smaller MHC-DP polymorphism than MHC-DQ or MHC-DR.

1. Introduction

Major histocompatibility complex (MHC) class II molecules display peptides on the surface of antigen-presenting cells (APC) for subsequent recognition by T cells, thereby performing a key defence role against pathogens. MHC class II molecules are heterodimers assembled from an α and a β glycopeptide chains encoded by the MHC class II A and B genes, respectively. Three main MHC class II loci, named HLA-DR, -DQ, and -DP, encode functional antigen-presenting molecules in primates. Genetic polymorphism and diversifying selection tied to functional and structural restrictions are common characteristics of these main loci. Such polymorphism is mainly restricted to the second exon of MHC class II A and B genes, constituting the molecule's peptide binding region (PBR) (Klein et al., 1993b).

MHC-DP is an ancient locus shared by divergent mammalian orders (Takahashi et al., 2000; Yuhki et al., 2003). However, its polymorphism and functionality vary. For example, MHC-DP acquires a pseudo-genic nature in felines, as also occurs in murinae (mouse-like rodents), even though MHC-DP is the most polymorphic MHC class II locus in other rodents, such as the mole rat (*Spalax* genus) (Klein et al., 1993a; Yuhki et al., 2003; Kelley et al., 2005).

MHC-DP is the most centromeric locus within the primate MHC gene cluster region, being constituted by four genes: DPA1 and DPB1 genes and DPA2 and DPB2 pseudogenes. This arrangement (position and number) is apparently the same in all primates and was established before the split between Platyrrhini and Catarrhini ~43 million years ago (MY) (Klein et al., 1993a; Steiper and Young, 2006).

MHC-DPA1 variability in primates varies amongst nonexistent and low polymorphism, whilst for MHC-DPB1, it fluctuates from moderate to high polymorphism (Otting and Bontrop, 1995; Slierendregt et al., 1995; Bontrop et al., 1999; Doxiadis et al., 2001). HLA-DPA1 exhibits low polymorphism in humans, where 28 alleles have been reported to date, compared to the 138 alleles described for HLA-DPB1 (Robinson, et al., 2003). In contrast, *Callithrix jacchus* (the common marmoset, a neo-tropical primate), has the MHC-DP region inactive, not expressing any MHC-DP molecule (Antunes et al., 1998). In spite of such low polymorphism, MHC-DPA1 can be important in modulating an immune response, since HLA-DPA1*0301 appears to be involved in the genetic susceptibility to *Schistosoma haematobium* and several chronic inflammatory diseases (May et al., 1998; Dai et al., 2010).

Previous studies have characterised *Aotus* MHC class II genes and molecules: MHC DQA-DQB (Diaz et al., 2000), MHC-DRB1 (Niño-Vasquez et al., 2000; Suarez et al., 2006), and MHC-DPB1 (Diaz et al., 2002). These neo-tropical primates have been shown to be susceptible to various human infectious diseases (Lujan et al., 1986; Polotsky

Abbreviations: MHC, Major histocompatibility complex; APC, antigen-presenting cells; PBR, peptide binding region; NWM, new world monkeys; OWM, old world monkeys; NJ, neighbour joining; ME, minimum-evolution; ML, maximum likelihood; LRSH, local rearrangements of tree topology around an edge; Pars, parsimony; GRMD, global rate minimum deformation method; MY, million years; SLAC, single likelihood ancestor counting; FEL, fixed effects likelihood; REL, random effects likelihood; Sub/S/MY, substitution per site per million years; TSP, trans-specific polymorphism.

* Corresponding author. Fundación Instituto de Inmunología de Colombia (FIDIC), Carrera 50 No. 26-20, Bogotá, Colombia. Tel.: +57 1 4815219; fax: +57 1 4815269.
E-mail address: mepatarr@gmail.com (M.E. Patarroyo).

0378-1119/$ – see front matter © 2010 Elsevier B.V. All rights reserved.
doi:10.1016/j.gene.2010.09.006

et al., 1994; Noya et al., 1998). They can develop human malaria, particularly *Plasmodium falciparum* (Gysin, 1988; Rodriguez et al., 1990; Collins, 1994) and *Plasmodium vivax* asexual/blood stage infections (Pico de Coana et al., 2003). This makes the owl monkey a highly valuable animal model for biomedical research. To complete this landmark, the study of MHC-DPA1 might play a key role in understanding the immune response against *Plasmodium* (Diaz et al., 2002) and contributes towards gaining a deeper knowledge about the immune system of owl monkeys. The exon 2 from *Aotus nancymaae* MHC-DPA1 gene was characterised to infer its allelic diversity, variability patterns, the amount and kind of its variation, the type of changes involved, as well as the extent of natural selection and evolutionary relationships within the primate context.

2. Materials and methods

2.1. Animals

Six *A. nancymaae* monkeys (4 males and 2 females) were randomly caught from different familiar groups in Lagos de Leticia and Atacuari River, two widely separated zones (80 km) in the Colombian Amazon. The monkeys were captured with the authorisation of the official environmental authority of Colombia in this region, CORPOAMAZONIA, which granted the Fundación Instituto de Inmunología de Colombia (FIDIC) permission for the capture, study, and scientific research with these primates in the Colombian Amazon (Resolutions #1966/2006 and 0028/2010 and previous authorisations beginning in 1982). This research has been performed following the guidelines approved by FIDIC's ethics committee. The studied animals have been always under the supervision of expert veterinarians and biologists, and after experimental procedures, they are released back into the Amazon jungle in optimal health conditions in the presence of a representative from CORPOAMAZONIA.

2.2. RNA extraction, cDNA synthesis, PCR, cloning, and sequencing

Leukocytes were obtained from six healthy *A. nancymaae* monkeys by density gradient separation of peripheral blood obtained by venous puncture. Total cellular RNA was isolated from peripheral blood mononuclear cells using the TRIzol one-step procedure (Invitrogen Life Technologies, CA, USA). Moloney murine leukaemia virus reverse transcriptase (Promega, Madison, WI, USA) was used for cDNA synthesis, according to the manufacturer's instructions.

Two PCR of MHC-DPA1 exon 2 were independently performed for each monkey; PCR primers used were GH98 (5′-CGCGGATCCTGTGTCAACTTATGCCGCG-3′) and GH99 (5′-CTGGCTGCAGTGTGGTTGGAACGCTG-3′) (Otting and Bontrop, 1995) at a final 0.8 μM concentration. The PCR mixture contained 1.5 μM $MgCl_2$, 50 mM Tris (pH 8.3) and 2.5 U Taq DNA polymerase (Promega). Five microlitres of cDNA was added to each reaction for a 25 μl final volume. These reactions were heated to 95 °C for 5 min and then amplified for 40 cycles as follows: denaturing for 30 s at 94 °C, annealing for 1 min at 65 °C, and extension for 2 min at 68 °C. A final extension cycle was run at 65 °C for 1 min and 68 °C for 5 min.

A WIZARD PCR Preps Purification kit (Promega) was used for purifying PCR products which were then ligated into pGEM T vector (Promega). MiniPreps Purification Kit (Mo Bio, Carlsbad, CA, USA) was used for isolating double-strand plasmid DNA. Three clones from each PCR were randomly chosen and sequenced using fluorescent dye-labelled dideoxy terminators (Applied Biosystems, Foster City, CA, USA) in an ABI Prism 310 genetic analyser (Applied Biosystems).

2.3. MHC-DPA1 sequences

A total of 64 exon 2 MHC-DPA1 gene sequences from 11 primates (suborder Anthropoidea) were used. **Platyrrhini** (new world monkeys (NWM)): *A. nancymaae*—owl monkey (*Aona*, 1 sequence, reported here) and *Saimiri sciureus*—squirrel monkey (Sasc, 3 sequences); **Catarrhini**: **Cercopithecidae** (old world monkeys—OWM): *Macaca arctoides*—stump-tailed macaque (Maar, 1 sequence), *Macaca fascicularis*—crab-eating macaque (Mafa, 6 sequences), *Macaca mulatta*—rhesus monkey (Mamu, 17 sequences), and *Papio hamadryas*—hamadryas baboon (Paha, 1 sequence); **Hominoidea** (humans and apes): *Homo sapiens*—human (HLA, 25 sequences), *Pan troglodytes*—chimpanzee (Patr, 3 sequences), *Gorilla gorilla*—gorilla (Gogo, 3 sequences), *Pongo pygmaeus*—Bornean orangutan (Popy, 3 sequences), and *Pongo abelii*—Sumatran orangutan (Poab, 1 sequence).

The following are the GenBank accession numbers of the studied sequences: Aona-DPA1*01—AF529200, Gogo-DPA1*0401—AF026701, Gogo-DPA1*0402—AF026702, Gogo-DPA1—CU104655, HLA-DPA1*010302—AF074848, HLA-DPA1*010304—DQ274060, HLA-DPA1*0104—X78198, HLA-DPA1*0105—X96984, HLA-DPA1*010601—U87556, HLA-DPA1*010602—EU729350, HLA-DPA1*0107—AF076284, HLA-DPA1*0108—AF346471, HLA-DPA1*0109—AY650051, HLA-DPA1*0110—DQ274061, HLA-DPA1*020101—X78199, HLA-DPA1*020102—L31624, HLA-DPA1*020103—AF015295, HLA-DPA1*020104—AF074847, HLA-DPA1*020105—AF098794, HLA-DPA1*020106—AF165160, HLA-DPA1*020203—AF092049, HLA-DPA1*02021—X79475, HLA-DPA1*02022—X79476, HLA-DPA1*0203—Z48473, HLA-DPA1*0204—EU304462, HLA-DPA1*0301—M83908, HLA-DPA1*0302—AF013767, HLA-DPA1*0303—AY618553, HLA-DPA1*0401—L11643, Maar-DPA1*0201—AF026703, Mafa-DPA1*0201—AF026704, Mafa-DPA1*0202—EF208806, Mafa-DPA1*0204—AM943632, Mafa-DPA1*0401—EF208808, Mafa-DPA1*0701—EF208809, Mafa-DPA1*0702—EF208810, Mamu-DPA1*0101—Z32411, Mamu-DPA1*0201—EF204945, Mamu-DPA1*0203—EF204950, Mamu-DPA1*0208—FJ544416, Mamu-DPA1*0401—FJ544417, Mamu-DPA1*0402—FJ544415, Mamu-DPA1*0403—GQ471885, Mamu-DPA1*0601—EF204949, Mamu-DPA1*0701—EF204946, Mamu-DPA1*0801—EU305663, Mamu-DPA1—AB219099, Mamu-DPA1—AB219100, Mamu-DPA1—AB219101, Mamu-DPA1—AB250754, Mamu-DPA1—AB250756, Mamu-DPA1—AB219102, Mamu-DPA1—AB250757, Paha-DPA1*0201—AF026706, Patr-DPA1*0201—AF026707, Patr-DPA1*0202—AF026693, Patr-DPA1*0301—AF026694, Poab-DPA1—AC207096, Popy-DPA1*0201—AF026695, Popy-DPA1*0202—AF026696, Popy-DPA1*0401—AF026697, Sasc-DPA1*0501—AF026698, Sasc-DPA1*0502—AF026699, Sasc-DPA1*0601—AF026700.

2.4. Sequence analysis

Clustal X (Thompson et al., 1997) was used for aligning the MHC-DPA1 exon 2 sequences. The *A. nancymaae* sequence was included and an amino acid alignment was also performed. HLA-DRA1*010101 and HLA-DQA1*010101 were used as outgroups. The resulting alignment had a total of 189/63 nucleotide/amino acid positions (Supplementary materials 1 and 2).

GENEDOC (Nicholas et al., 1997) was used for calculating the percent of identity (i.e., equal positions between sequences) and similarity (i.e., positions with conservative substitutions between sequences, in this case, assessed by the PAM 250 substitution matrix) in the considered alignments. Means and standard deviations of pairwise nucleotide and amino acid identity and similarity (this last one for amino acid sequences only) inside each group of sequences were analytically calculated.

Each position's variation for MHC-DPA1 exon 2 amino acid aligned sequences was represented by using WebLogo (Crooks et al., 2004). All amino acids occupying each position were indicated, in which the height of every amino acid letter represented its relative frequency in that position. The logo also allowed conservative and nonconservative substitutions for each position to be determined, where the variation in an amino acid symbol's colour indicated nonconservative changes and its preservation represented conservative changes based on PAM

250 substitution matrix groups (DENQH/ SAT/ KR/ FYW/ LIVM/ C/ G and P) (Dayhoff et al., 1978).

2.5. Phylogenetic analysis

Neighbour Joining (NJ) and Minimum evolution (ME) (Rzhetsky and Nei, 1993) trees were constructed using MEGA 4.0 (Tamura et al., 2007). Genetic distances were estimated by using Kimura 2-parameter (Kimura, 1980), Log-Det (Tamura and Kumar, 2002) and Maximum Composite Likelihood (Tamura et al., 2004) substitution models for nucleotide sequences and JTT (Jones et al., 1992) and Dayhoff (Schwarz and Dayhoff, 1979) substitution models for amino acid-deduced sequences. Bootstrap analysis (Hillis and Bull, 1993) and interior branch test (IBT) (Sitnikova, 1996), both with 10,000 replicates, were used for assigning confidence levels to branch nodes. Nodes having bootstrap values greater than 70% were statistically significant, as well as internal branch test values greater than 95%.

Maximum likelihood (ML) (Felsenstein, 1981) trees were constructed using TREEFINDER (Jobb et al., 2004) and DNAML / PROTML included in the PHYLIP package (Felsenstein, 1989); Bootstrap analysis (Hillis and Bull, 1993), with 10,000 replicates, was used for assigning confidence levels to branch nodes. Genetic distances for TREEFINDER were calculated by using the estimated model from data following AICc criteria, in this case, HKY (Hasegawa et al., 1985) substitution model for nucleotide sequences and JTT (Jones et al., 1992) substitution model for amino acid sequences. Bootstrap analysis (Hillis and Bull, 1993) and local rearrangements of tree topology around an edge (LRSH) (Shimodaira and Hasegawa, 1999), both having 10,000 replicates, were used for assigning confidence levels to branch nodes. Nodes having LRSH values greater than 95% were considered statistically significant.

Parsimony (Pars) (Felsenstein, 1983) trees were constructed using MEGA 4.0 (Tamura et al., 2007) and DNAPARS, both included in the PHYLIP package (Felsenstein, 1989). Bootstrap analysis (Hillis and Bull, 1993), with 10,000 replicates, was used for assigning confidence levels to branch nodes.

A Bayesian approach was also used for inferring phylogenetic relationships using MrBayes (Ronquist and Huelsenbeck, 2003). Default settings for the GTR model with gamma-distributed rate variation across sites and a proportion of invariable sites for nucleotide sequences and a mixed model for amino acid sequences, were used. Two simultaneous Markov chain Monte Carlo analyses were performed using one cold and three heated chains (temperature set to default 0.2) for each analysis. Simulations were run for 15,000,000 generations with a tree being saved each 100th generation. At approximately 10 million generations for the nucleotide alignment and 11 million generations for the amino acid alignment, the standard deviation of split frequencies reached a <0.01 value, indicating that both analyses converged on similar trees. The last 25% generations were preserved as burn-in and generated a consensus tree. Nodes having posterior probability values of 85–89 were considered to have low statistical support, 90–94 to have moderate support, and nodes greater than 95 to be highly supported (Huelsenbeck and Ronquist, 2001).

2.6. Tree calibration

Global Rate Minimum Deformation method (GRMD), implemented in TREEFINDER software (Jobb et al., 2004), was used to estimate the evolutionary rates of DPA groups deduced from the Bayesian tree (calculated in MrBayes for nucleotide sequences). As calibration points, the divergence time amongst Catarrhini–Platyrrhini = 42.9 million years (MY) (36.1–51.1 MY), Platyrrhini–Platyrrhini = 21.0 MY (19.15–22.05 MY), Catarrhini–Catarrhini = 30.5 MY (26.9–36.4 MY), Hominoidea–Hominoidea = 18.3 MY (16.3–20.8 MY), *Homo–Pan* = 6.6 MY (6–7 MY), *M. mulatta–M. fascicularis* = 0.9 MY were used (Goodman et al., 1998; Opazo et al., 2006; Osada et al., 2008).

2.7. Natural selection analysis

Natural selection was detected using single likelihood ancestor counting (SLAC), fixed effects likelihood (FEL) and random effects likelihood (REL) methods using HYPHY (Kosakovsky-Pond et al., 2005). These maximum likelihood-based methods estimated the rates of nonsynonymous and synonymous changes at each site in the sequence alignment and identified sites under positive or negative selection (Kosakovsky-Pond and Muse, 2005; Kosakovsky-Pond and Frost, 2005b). For SLAC and FEL methods, a p value ≤ 0.1, whilst for REL, the Bayes factor ≥ 50 were considered as significant. The algorithms are available on the Datamonkey Web (Kosakovsky-Pond and Frost, 2005a; Poon et al., 2009). Also MEGA 4.0 software was used for calculating synonymous and nonsynonymous substitutions and associated variance rates (assessed by the bootstrap method with 1000 replicates) by Nei–Gojobori's method (Nei and Gojobori, 1986).

2.8. 3D representations

Positions under variation/selection were represented in a 3D model of each Pocket (including adjacent residues within a range of 5 Å) for DPA, from crystallized DPA1 complex (PDB 3LQZ from DPA1*0103–DPB1*0201) (Dai, et al., 2010) using VMD 1.87 (Humphrey et al., 1996).

3. Results

3.1. MHC Aona-DPA1 sequence

The MHC-DPA1 exon 2 from six *A. nancymaae* monkeys was amplified by RT–PCR. Amplification products had a 189 bp size, corresponding to exon 2 positions 34–222 (12–74 in α domain). A total of 36 clones were sequenced yielding an identical sequence. Analysed sequences, including the Aona-DPA1 sequence, are shown in Supplementary material 1 (Exon 2) and Supplementary material 2 (α domain).

3.2. Evolutionary analysis of Aona-DPA1 exon 2

Independently of the tree construction method (Bayesian, Parsimony, NJ, ME, or ML) or the substitution model assumed, MHC-DPA1 exon 2 sequences analysed clustered into similar groups. For the sake of simplicity, five MHC-DPA1 groups were defined (Fig. 1): Group 1, supported by a high posterior probability value and LRSH value, formed by alleles DPA1*05 and DPA1*07 from all Anthropoidea groups, including the *A. nancymaae* DPA sequence. MHC Aona-DPA1 was clearly included in MHC-DPA1*05 lineage, having high statistically supported values in all phylogenetic methods used. Group 2, supported by LRSH, formed mainly by DPA1*01 and DPA1*03 alleles from Catarrhini groups, but mainly conformed by human sequences. Group 3, formed mainly by HLA-DPA1*02 sequences and supported by LRSH. Group 4 contains sequences from all Anthropoidea groups distributed in four well-supported subgroups: DPA1*04 from Hominoidea; DPA1*04 from Cercopithecidae; DPA1*06 from *S. sciureus* (Platyrrhini) and *M. mulatta* (Cercopithecidae) and a subgroup conformed of two unnamed alleles from *M. mulattta*. Group five comprises Catarrhini sequences, primarily DPA1*02 sequences from Cercopithecidae and also DPA1*02 from *P. pygmaeus*. All group associations were relatively well conserved at protein-deduced sequence level, but some not so well supported (data not shown). Groups 1, 2, 4, and 5 displayed a trans-species or convergent nature (Fig. 1). Moreover, some sequences were identical amongst species.

3.3. Evolutionary rate estimation in primate MHC-DPA1 exon 2

Aona-DPA1*01 exon 2 appears as one of the most divergent sequence amongst primate MHC-DPA1 sequences. A tree calibration was carried out in order to establish whether divergence corresponds to a high evolutionary rate or corresponds to a long time of existence

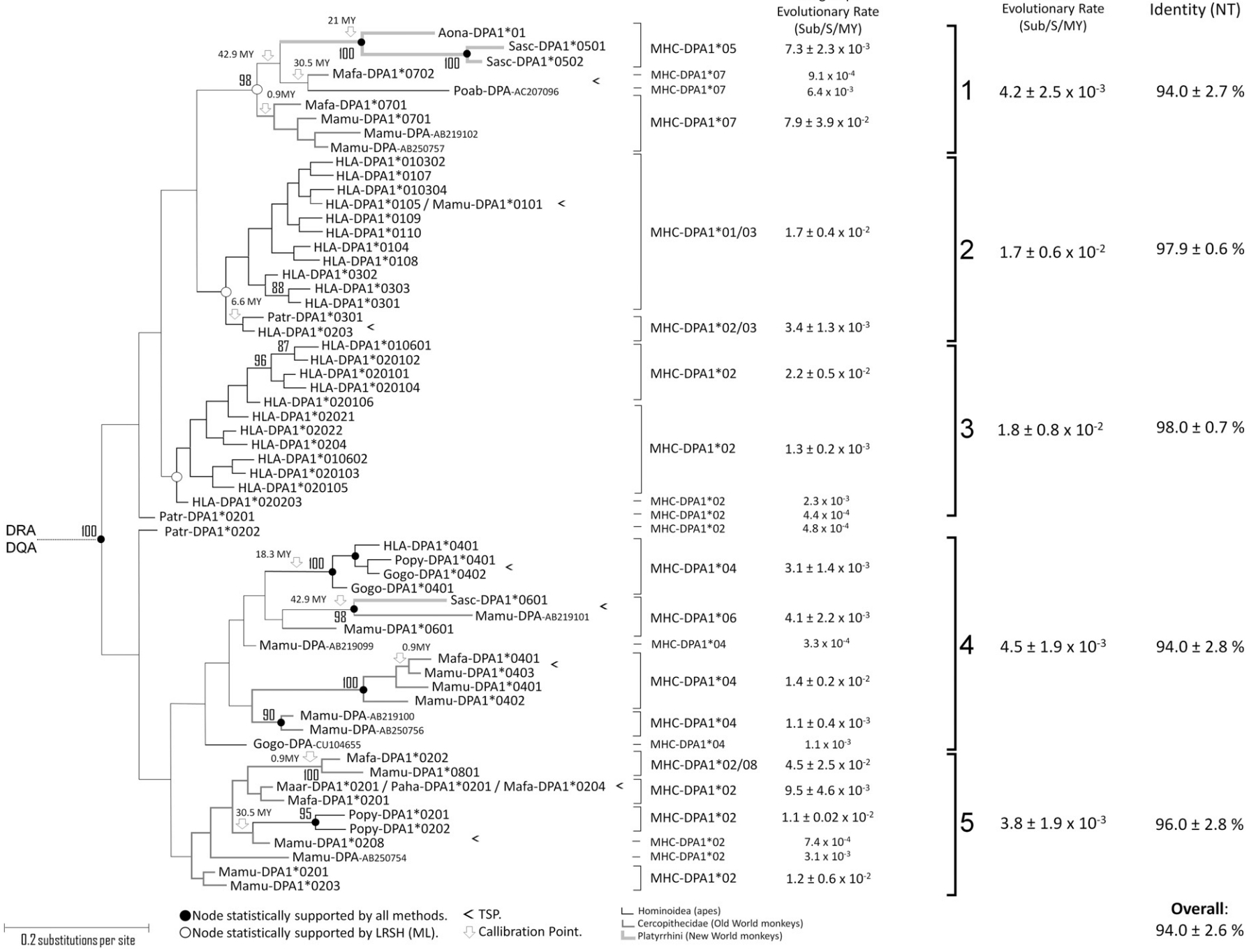
Subgroups Evolutionary Rate (Sub/S/MY)
Groups Evolutionary Rate (Sub/S/MY)
Identity (NT)
21 MY
Aona-DPA1*01
Sasc-DPA1*0501
Sasc-DPA1*0502
42.9 MY
30.5 MY
Mafa-DPA1*0702
Poab-DPA-AC207096
0.9MY
Mafa-DPA1*0701
Mamu-DPA1*0701
Mamu-DPA-AB219102
Mamu-DPA-AB250757
HLA-DPA1*010302
HLA-DPA1*0107
HLA-DPA1*010304
HLA-DPA1*0105 / Mamu-DPA1*0101
HLA-DPA1*0109
HLA-DPA1*0110
HLA-DPA1*0104
HLA-DPA1*0108
HLA-DPA1*0302
HLA-DPA1*0303
HLA-DPA1*0301
6.6 MY
Patr-DPA1*0301
HLA-DPA1*0203
HLA-DPA1*010601
HLA-DPA1*020102
HLA-DPA1*020101
HLA-DPA1*020104
HLA-DPA1*020106
HLA-DPA1*02021
HLA-DPA1*02022
HLA-DPA1*0204
HLA-DPA1*010602
HLA-DPA1*020103
HLA-DPA1*020105
HLA-DPA1*020203
Patr-DPA1*0201
DRA
DQA
Patr-DPA1*0202
HLA-DPA1*0401
18.3 MY
Popy-DPA1*0401
Gogo-DPA1*0402
Gogo-DPA1*0401
Sasc-DPA1*0601
42.9 MY
Mamu-DPA-AB219101
Mamu-DPA1*0601
Mamu-DPA-AB219099
0.9MY
Mafa-DPA1*0401
Mamu-DPA1*0403
Mamu-DPA1*0401
Mamu-DPA1*0402
Mamu-DPA-AB219100
Mamu-DPA-AB250756
Gogo-DPA-CU104655
0.9MY
Mafa-DPA1*0202
Mamu-DPA1*0801
Maar-DPA1*0201 / Paha-DPA1*0201 / Mafa-DPA1*0204
Mafa-DPA1*0201
30.5 MY
Popy-DPA1*0201
Popy-DPA1*0202
Mamu-DPA1*0208
Mamu-DPA-AB250754
Mamu-DPA1*0201
Mamu-DPA1*0203
MHC-DPA1*05
7.3 ± 2.3 x 10-3
MHC-DPA1*07
9.1 x 10-4
MHC-DPA1*07
6.4 x 10-3
MHC-DPA1*07
7.9 ± 3.9 x 10-2
MHC-DPA1*01/03
1.7 ± 0.4 x 10-2
MHC-DPA1*02/03
3.4 ± 1.3 x 10-3
MHC-DPA1*02
2.2 ± 0.5 x 10-2
MHC-DPA1*02
1.3 ± 0.2 x 10-3
MHC-DPA1*02
2.3 x 10-3
MHC-DPA1*02
4.4 x 10-4
MHC-DPA1*02
4.8 x 10-4
MHC-DPA1*04
3.1 ± 1.4 x 10-3
MHC-DPA1*06
4.1 ± 2.2 x 10-3
MHC-DPA1*04
3.3 x 10-4
MHC-DPA1*04
1.4 ± 0.2 x 10-2
MHC-DPA1*04
1.1 ± 0.4 x 10-3
MHC-DPA1*04
1.1 x 10-3
MHC-DPA1*02/08
4.5 ± 2.5 x 10-2
MHC-DPA1*02
9.5 ± 4.6 x 10-3
MHC-DPA1*02
1.1 ± 0.02 x 10-2
MHC-DPA1*02
7.4 x 10-4
MHC-DPA1*02
3.1 x 10-3
MHC-DPA1*02
1.2 ± 0.6 x 10-2
1
4.2 ± 2.5 x 10-3
94.0 ± 2.7 %
2
1.7 ± 0.6 x 10-2
97.9 ± 0.6 %
3
1.8 ± 0.8 x 10-2
98.0 ± 0.7 %
4
4.5 ± 1.9 x 10-3
94.0 ± 2.8 %
5
3.8 ± 1.9 x 10-3
96.0 ± 2.8 %
Overall:
94.0 ± 2.6 %
0.2 substitutions per site
Node statistically supported by all methods.
Node statistically supported by LRSH (ML).
TSP.
Callibration Point.
Hominoidea (apes)
Cercopithecidae (Old World monkeys)
Platyrrhini (New World monkeys)

(Fig. 1). For sake of simplicity, it has been assumed that the divergence times used as calibration points for MHC-DPA1 exon 2, correspond to the divergence time amongst species. As can be seen, primate MHC-DPA1 groups are divided in two tendencies: groups 1, 4, and 5 have similar rates, between 3.8 and 4.5×10^{-3} Sub/S/MY, evolving about 4 – 4.5 times slower than groups 2 and 3, which have a rate between 1.7 and 1.8×10^{-2} Sub/S/MY.

Within groups, the rates are often very variable. For example, in group 1, the subgroup MHC-DPA1*05 is formed by Sasc-DPA1*0501, *0502, and Aona-DPA1*01, with an evolutionary rate about 10 times slower than the rate of the subgroup formed by sequences from *Macaca* MHC-DPA1*07, being the rate of this group the highest observed in the analysis (7.3×10^{-3} vs. 7.9×10^{-2} Sub/S/MY). In contrast, Mafa-DPA1*0702 shows the lowest evolutionary rate observed (9.1×10^{-4} Sub/S/MY). This pattern of variability occurs within all groups considered. The different evolutionary constrains amongst alleles and species may be reflected by the rate variation within and amongst the studied groups.

3.4. Primate MHC-DPA1 exon 2 variability

Overall identity at nucleotide level was high, having a 94% mean (88%–100% range) (Fig. 1). The logo of the deduced amino acid sequence of MHC-DPA1 α domain for the set of all analysed species which was remarkably conserved, having 95.1% mean similarity (88%–100% range) and 90.7% identity (75%–100% range) (Fig. 2). In general, most amino acid substitutions were nonconservative (24 from 33 variable positions) considering all sequences analysed (Anthropoidea DPA, Fig. 2). Groups 1 and 4 displayed a greater amount of sequence variability, followed by group 5, whereas the remaining lineages showed a most conservative nature (at nucleotide and amino acid identity and at amino acid similarity, Figs. 1 and 2).

Aona-DPA1 possessed distinctive nucleotide and amino-acid substitutions (16Q→H, 31I→M, 54V→F, 56V→A, 65A→I), being the most nonconservative (Fig. 2, Supplementary materials 1 and 2). This characteristic highlights its divergent nature, shared with other NWM-DPA sequences.

Most variable positions at nucleotide and amino acid levels were grouped within positions 50 and 74 in amino acid sequence (150 and 222 in nucleotide sequence, red line in Fig. 2). This sector includes most of the residues involved in the interaction with peptide (Pocket residues) at PBR, as assigned by homology with HLA-DPA1*0103 (Dai et al., 2010). The region between amino acids 12 and 49 was more conserved (34–150 in nucleotide sequence, black line in Fig. 2).

The variability of MHC-DPA1 exon 2 is concentrated especially in Pocket residues and their neighbours. The most variable is the Pocket 9, followed by Pockets 6 and 1. Each group varies in a distinct way at Pocket level, i.e., for both nucleotide and amino acids, group 4 is the most variable at Pocket 1, group 5 is the most variable at Pocket 6, group 1 is the most variable at Pocket 9 and group 3 only varies at Pocket 9 (Fig. 2). The substitution pattern at the codon level in the PBR is concentrated in first and second positions in all groups, with the exception of group 4, in which all codon positions exhibit equivalent variability. In the remaining sequences, substitutions in the third codon position prevail (supplementary material 3).

3.5. Natural selection in primate MHC-DPA1 exon 2

No complete correspondence between SLAC, FEL, and REL selection tests for all the analysed positions was observed, only some common positions being detected (Fig. 2 and Supplementary material 4). MHC-DPA1 exon 2 for the set of all analysed groups displayed an accumulation of negatively selected positions (when present) in the less variable region (codons 12–49) and an accumulation of positively selected positions (when present) in the most variable region (codons 50–74). This pattern also occurred in most MHC-DPA1 groups (with the exception of group 5). With a few exceptions, no common positions under selection occurred between groups. Pocket positions assigned by homology (Dai et al., 2010) and near residues showed greater variability, accumulation of nonsynonymous and nonconservative substitutions and, in some cases, are under positive selection. Positions submitted to negative selection tend to occur with greater frequency in non-PBR sectors, as has been reported previously (Hughes and Yeager, 1998) (Fig. 2).

All Pockets suffer selective pressures, but not in the same way depending on the group. Groups 1 and 2 show more positions under positive selection than the other lineages analysed (seven of seven in group 2, seven of eight in group 1), but in group 1, those positions are more variable than the observed in group 2, and comprise Pockets 6 and 9. On the other hand, group 2 shows selective forces in Pockets 1, 6, and 9. Groups 3 and 4 show only positions under negative selection, and in both groups, these positions occur outside the Pockets. Group 5 Pockets 1 and 6 are under positive selection, having this group more positively selected positions in the less variable sector, and two of these positions occur at the Pockets 1 and 6. The result of the analysis of all sequences together (Anthropoidea DPA) shows the occurrence of positively selected positions (four of seven) interspersed amongst the negatively selected positions in the less variable sector of the molecule. Two of them occur in residues with potential contact with the peptide (13 and 42) and two in Pocket residues (23 and 31). No positions under negative selection pressure were observed in Pocket residues. The remaining positions under positive selection occur in the most variable region, at Pocket 9 (72 and 73) and at a neighbour residue (68).

A detailed analysis of positions under variation and/or selection for MHC-DPA1 has been performed (Fig. 3). Considering all positions under selection for groups and sequences together, all Pockets are under positive pressure (Figs. 3A, C, E), and that condition might be extended to some neighbour residues (considered as residues in direct contact with Pocket residues, at distances <5 Å; Figs. 3B, D, F). In Pocket 1, the definition of neighbour comprises the major number of residues amongst DPA1 Pockets, showing all possible tendencies. Six neighbour positions are under positive selection (in red) and two are variable (green) in positions that might involve peptide contact (Fig. 3B). Some of these positions are considered Pocket residues in DRA locus (Stern et al., 1994; Cardenas et al., 2004). Pocket 1 is highly conserved amongst DPA1 sequences analysed (Fig. 2), showing the nonvariant residue α32F (blue) and negatively selected neighbour positions (ice blue) (Figs. 3A and B, respectively). Despite its conservation, the subtle variation observed is a consequence of diversifying forces. Pocket 6 shows six variable neighbour positions above the Pocket residues and a negatively selected position in the Pocket base alongside a positively selected position (Fig. 3D). Pocket 6 is also highly conserved, but less than Pocket 1, showing variable positions such as α31 (Fig. 2). Pocket 9 is the most variable amongst Pockets considered, showing variable positions as 69, 72, and 73, all under positive selection (Figs. 2 and 3E). Only one neighbour position shows high variability and positive pressure, (α68), and as in the previous cases, it is considered Pocket position for DRA loci.

Nei–Gojobori's method confirms these results, showing a significant accumulation of nonsynonymous substitutions in PBR region for

Fig. 1. Phylogenetic tree calculated using a Bayesian approach for primate MHC-DPA1 exon 2 sequences. Topologies obtained for parsimony (Pars), maximum likelihood (ML), and minimum evolution (ME) are similar, and significant node support from these analyses is also shown (Bootstrap >70%; IBT >90%, LRSH >95%; see the code at the bottom of the figure). Primate species divergence time in million years (MY) and mean substitution per site per million years (Sub/S/My) are shown for each group and subgroup, the average nucleotide identity obtained from all possible pairwise comparisons of exon 2 is also shown. The scale indicates 0.2 substitutions per site. See Materials and methods section for species abbreviations and calculation details.

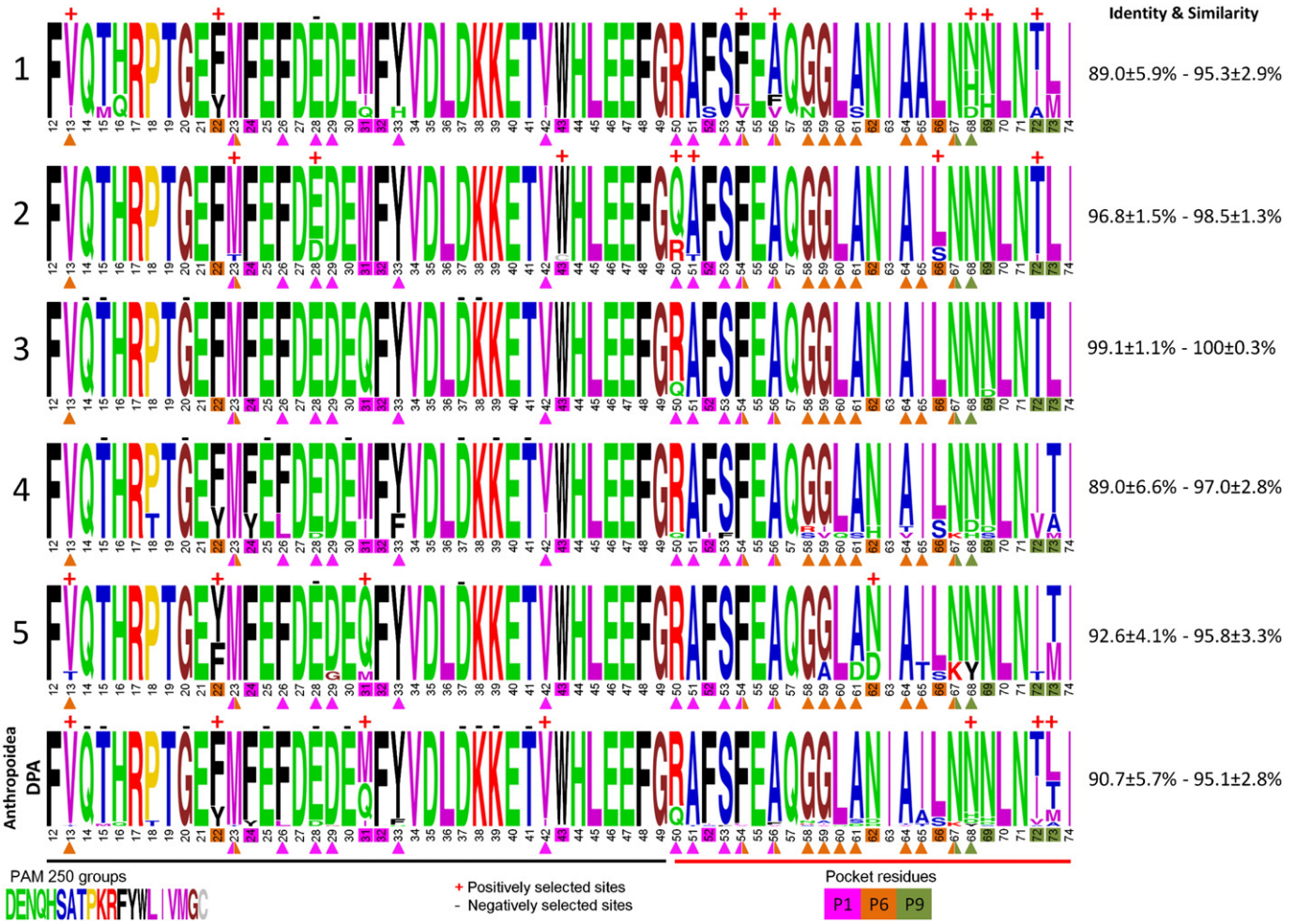

Fig. 2. MHC-DPA1 exon 2-deduced amino acid sequence logo. PAM 250 substitution matrix groups (DENQH (green), SAT (blue), KR (red), FYW (black), LIVM (purple), C (gray), G (brown), and P (yellow)) are used to show conservative or nonconservative substitutions; colour changes imply non-conservative substitutions. Above each logo, sites under positive selection (combined results for SLAC, FEL and REL tests) are marked with +, whilst those under negative selection are shown with − ; the remaining sites are unmarked and are considered neutral. Coloured numbers below each logo denote Pocket positions: fuchsia P1, orange P6, green P9, coloured arrows indicate other residues in contact with Pocket residues. At the right-hand side, the amino acid identity and amino acid similarity in primate MHC-DPA1 are shown. The average was obtained from all possible pairwise comparisons of deduced MHC-DPA1 protein sequences within each group. Similarity was calculated based on PAM 250 substitution matrix.

all sequences together; groups 1, 2, and 5 show significant positive selection in PBR, group 3 shows a near neutral substitution pattern, and group 4 shows a nonsignificant accumulation of synonymous vs. nonsynonymous substitutions. The non-PBR region displays the opposite behaviour, showing a significant accumulation of synonymous vs. nonsynonymous substitutions for all sequences together; groups 3 and 4 show significant negative selection in this region, whilst the remaining groups show the same tendency but statistically unsupported. When analysing the entire sequence, all DPA1 groups and all DPA1 sequences together show accumulation of synonymous vs. nonsynonymous substitutions, being significant only for group 3. In the less variable region (codons 12–49), all groups display the same pattern, and groups 3, 4, and 5 show a significant negative selection. In the most variable region (codons 50–74), all groups show more nonsynonymous than synonymous substitutions, but without statistical support (Supplementary materials 3 and 5).

4. Discussion

The study of MHC-DPA1 represents an essential task in order to improve our understanding of both the MHC class II and the immune system in the owl monkey. The central role of MHC class II in defence against pathogens and its continuous struggle with changing pathogen strategies has caused a complex evolutionary scenario, in which multiple factors such as adaptive evolution by overdominance, gene conversion, intra-allelic recombination, and other recombination processes have shaped MHC polymorphism. The degree of polymorphism varies between MHC loci, as a result of different functional constrains (adaptive diversification or conservation), and stochastic processes (such as a bottleneck in population structure); these differences became relevant when comparing different immune systems (Hughes and Yeager, 1998; Bontrop et al., 1999; Yuhki et al., 2003).

A. nancymaae MHC class II polymorphism and evolutionary relationships have been previously explored using similar strategies to those used in this article. In the case of MHC-DQ, Diaz et al. (2000) found 5 MHC-DQA1 (Aona-DQA1*27) alleles isolated from 3 owl monkeys, 14 MHC-DQB1 (Aona-DQB1*22 and Aona-DQB1*23) alleles, and 2 Aona-DQB2 alleles isolated from 19 monkeys. Suarez et al. (2006) have found 98 alleles for MHC-DRB (split into 12 lineages) isolated from 86 owl monkeys and Diaz et al. (2002) reported 3 alleles for MHC-DPB1 isolated from 7 owl monkeys.

This work reports one Aona-DPA1 sequence isolated from 6 owl monkeys, suggesting that Aona-DPA1 may display a limited or non-existent polymorphism. Aona-DPA1 constitutes a divergent sequence located in one of the most variable groups within the context of primate MHC-DPA1. Despite the MHC-DPA1*05 lineage support, internal

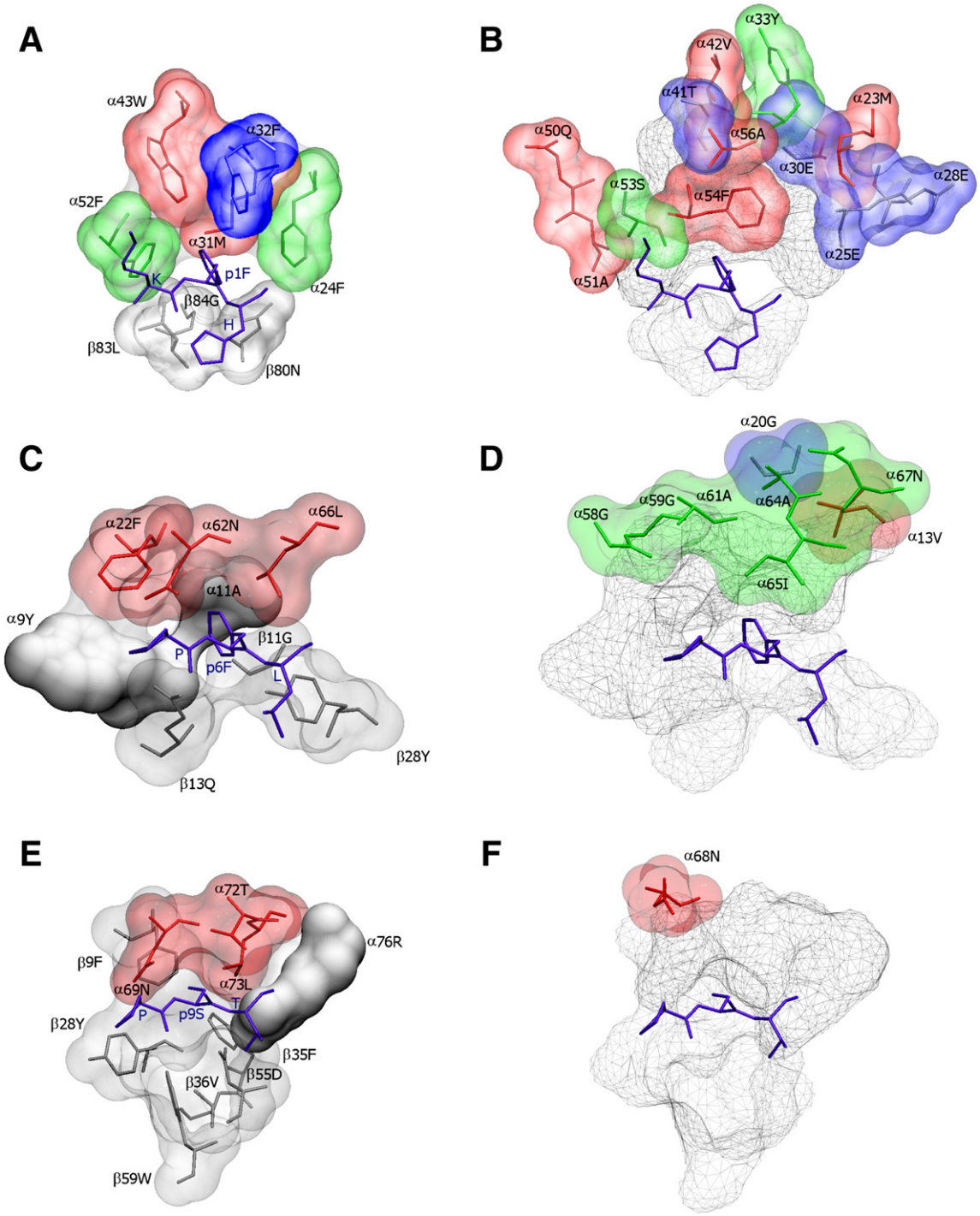

Fig. 3. Pockets of MHC-DPA1. Based in the PDB 3LQZ (DPA1*0103, DPB1*0201), the pockets and their neighbouring residues are shown: (A) Pocket 1, (B) Pocket 1 neighbour residues, (C) Pocket 6, (D) Pocket 6 neighbour residues, (E) Pocket 9 and (F) Pocket 9 neighbour residues. Red indicates positively selected residues; ice blue, negatively selected residues; blue, invariant residues; green, variable residues; and white, nonconsidered residues.

similarity and identity were often lower than similarity and identity observed between Aona-DPA1 and other MHC-DPA1 sequences from different loci (not shown). However, they share exclusive substitutions (Supplementary material 1 and Fig. 2). Such high variability is caused by the age of the group, and it has also been associated with greater variable positions and nonconservative changes; when high positively selected positions are added up to these findings (Fig. 2), particular functional constrains might be inferred for the evolution of this group.

The most polymorphic locus in the owl monkey, as in humans and other primates, is thus MHC-DR. Such polymorphism is concentrated in MHC-DRB, whilst MHC-DRA is conserved in the studied primates. MHC-DRB is the only polymorphic gene in the common marmoset (*C. jacchus*) (Antunes et al., 1998; Bontrop et al., 1999).

The second most polymorphic MHC class II locus varies between different species; it is MHC-DQ for the owl monkey and rhesus monkey (*M. mulatta*), whereas it is MHC-DP for humans. The least

variable locus is MHC-DP for the owl monkey and rhesus monkey (Slierendregt et al., 1995), and in humans, it is MHC-DQ (Bontrop et al., 1999; Robinson et al., 2003).

Although more sampling may be necessary, these results support *A. nancymaae* as having a smaller polymorphism in MHC-DP than in MHC-DQ or MHC-DR. These data establish differences between *Aotus* and *Callithrix*, denoting the different MHC class II restrictions and specialisation in new world monkeys, and in a global view, the different strategies used by each primate species regarding the specialisation and diversification of their MHC class II repertories.

The existence of trans-species polymorphism (TSP) has been well established for several MHC loci in primates (Klein, 1987; Klein et al., 1998), but it can be mimicked by molecular convergence phenomena, as established for exon 2 from DRB1, DQA, DQB, and DPB MHC class II genes (O'HUigin, 1995; Trtkova et al., 1995; Kriener et al., 2000a, b, 2001). All the above shows that only trans-species polymorphism has been found within Anthropoidea infraorders such as Catarrhini and Platyrrhini. If the TSP occurs, its duration is greater in MHC-DPA1 than MCH-DPB1, as can be observed in *A. nancymaae* (Diaz et al., 2002) and in other primates (Otting and Bontrop, 1995).

Association between Aona-DPA1 and Sasc-DPA1*05 in a highly supported NWM clade (Fig. 1) becomes a trans-specific lineage. Other Catarrhini-exclusive trans-specific MHC-DPA1 lineages have been detected (Fig. 2). Group 1, formed by MHC-DPA1*05 and MHC-DPA1*07, includes Catarrhini sequences from *Pongo* and *Macaca*. This indicates the noticeable antiquity of this group, being the best supported clade in primate order. This group and MHC-DPA1*06 lineage (group 4) show long evolutionary times, predating the divergence between Catarrhini and Platyrrhini. The absence of Platyrrhini sequences in the other groups might obey to the small sampling of MHC-DPA1 in these primates. Interestingly, human, the best sampled primate, restricts most of its allelic repertoire to two groups (2 and 3) with a high conservation but also a high evolutionary rate. The evolutionary significance of this apparent specialisation may be explained by the birth and death model (Takahashi et al., 2000; Piontkivska and Nei, 2003) or by the origin of sequences, frequently derived from expressed genes only. In group 2, an almost human lineage (with the exception of Patr-DPA1*0301), the virtual identity amongst HLA-DPA1*05 and Mamu-DPA1*0101 may indicate the existence of an ancient TSP or a molecular convergence. Interestingly, this lineage shows a high number of positively selected positions, indicating a strong process of diversifying selection within the human lineage. These results show not only the existence of MHC-DPA specific lineages in some primate clades but also long-term lineages as group 1 or MHC-DPA1*06 in group 4. This emphasises the need for a greater sampling amongst primate species to better understand MHC-DPA evolution.

In spite of its low variation, MHC-DPA1 exon 2 displayed differential variability constrains along the sequence, exhibiting a conserved region (residues 12–49) in which synonymous substitutions and negatively selected positions prevailed, and a mostly variable region (residues 50–74) in which nonsynonymous substitutions and positively selected positions predominated (Fig. 2). This observation may have functional relevance indicating compartmentalisation. As other MHC genes, the positive selection is focused on PBR positions, and negative selection occurs on non-PBR positions; however, all groups analysed show specific variation and selection patterns, e.g., group 1 shows a relatively high sequence diversity, a slow evolutionary rate, and predominance of diversifying selection; group 4 also shows a relatively high diversity and slow evolutionary rate, but evidence of purifying selection, explained by the accumulation of substitutions in the third position of the codon that lead to accumulating synonymous substitutions. On the other hand, group 2 shows a relatively low diversity and a high evolutionary rate as group 3, but group 2 shows evidence of a diversifying selection whilst group 3 displays evidence of a purifying selection. These differences amongst groups also involve the Pockets themselves, being stressed to different selection patterns depending on the group. All the above suggests the existence of differences between the evolutionary restrictions modelling the peptide binding boundaries for each group analysed.

The detection of variation and selective constrains beyond the Pocket residues may have a functional importance. In some cases, those positions might be involved in peptide contact or in the modification of electrostatic properties of the Pocket by surrounding residues (Fig. 3). The visualisation of that "extended Pockets" suggests that the binding interactions described by crystallographic studies might be fuzzier, and the evolutionary analysis provides evidence of different binding capacities for noncrystallised alleles. These subtle residue variations might be functionally relevant, as has been described in other MHC contexts (Posch et al., 1995; Posch et al., 1996).

The above results led us to conclude that Aona-DPA1 shows a limited or nonexistent polymorphism and is associated with Sasc-DPA1*05, forming a strongly supported lineage with distinctive variability and selective patterns from the other primate–MHC-DPA1 lineages. Our results show differences in the evolutionary pattern of HLA-DPA, suggesting a recent but strong diversifying process in the human lineage. The groups delimited from our analyses possess a set of distinctive features at diversity and selection patterns, indicating several modes of evolution in primate MHC-DPA.

Supplementary data to this article can be found online at doi:10.1016/j.gene.2010.09.006.

Acknowledgments

This work was funded by COLCIENCIAS, contract RC-140-2009. We would like to thank Monica Estupiñan for laboratory technical support in the obtaining of sequences and Gisselle Rivera for helping in the translation of this manuscript.

References

Antunes, S.G., De Groot, N.G., Brok, H., Doxiadis, G., Menezes, A.A., Otting, N., et al., 1998. The common marmoset: a new world primate species with limited MHC class II variability. Proc. Natl Acad. Sci. USA 95, 11745–11750.

Bontrop, R.E., Otting, N., De Groot, N.G., Doxiadis, G.G., 1999. Major histocompatibility complex class II polymorphisms in primates. Immunol. Rev. 167, 339–350.

Cardenas, C., Villaveces, J.L., Bohorquez, H., Llanos, E., Suarez, C., Obregon, M., et al., 2004. Quantum chemical analysis explains hemagglutinin peptide–MHC class II molecule HLA-DRbeta1*0101 interactions. Biochem. Biophys. Res. Commun. 323, 1265–1277.

Collins, W.E., 1994. The owl monkey as a model for malaria. In: Baer, W.K. (Ed.), *Aotus*: The Owl Monkey. Academic Press, pp. 245–258.

Crooks, G.E., Hon, G., Chandonia, J.M., Brenner, S.E., 2004. WebLogo: a sequence logo generator. Genome Res. 14, 1188–1190.

Dai, S., Murphy, G.A., Crawford, F., Mack, D.G., Falta, M.T., Marrack, P., et al., 2010. Crystal structure of HLA-DP2 and implications for chronic beryllium disease. Proc. Natl Acad. Sci. USA 107, 7425–7430.

Dayhoff, M.O., Schwartz, R.M., Orcutt, B., 1978. A model of evolutionary change in proteins. In: Dayhoff, M. (Ed.), Atlas of Protein Sequence and Structure. National Biomedical Research Foundation, pp. 345–352.

Diaz, D., Naegeli, M., Rodriguez, R., Nino-Vasquez, J.J., Moreno, A., Patarroyo, M.E., et al., 2000. Sequence and diversity of MHC DQA and DQB genes of the owl monkey *Aotus nancymaae*. Immunogenetics 51, 528–537.

Diaz, D., Daubenberger, C.A., Zalac, T., Rodriguez, R., Patarroyo, M.E., 2002. Sequence and expression of MHC-DPB1 molecules of the new world monkey *Aotus nancymaae*, a primate model for *Plasmodium falciparum*. Immunogenetics 54, 251–259.

Doxiadis, G.G., Otting, N., De Groot, N.G., Bontrop, R.E., 2001. Differential evolutionary MHC class II strategies in humans and rhesus macaques: relevance for biomedical studies. Immunol. Rev. 183, 76–85.

Felsenstein, J., 1981. Evolutionary trees from DNA sequences: a maximum likelihood approach. J. Mol. Evol. 17, 368–376.

Felsenstein, J., 1983. Parsimony in systematics. Biol. Stat. Ann. Rev. Ecol. Syst. 313–333.

Felsenstein, J., 1989. PHYLIP - Phylogeny Inference Package (Version 3.2). Cladistics, pp. 164–166.

Goodman, M., Porter, C.A., Czelusniak, J., Page, S.L., Schneider, H., Shoshani, J., et al., 1998. Toward a phylogenetic classification of primates based on DNA evidence complemented by fossil evidence. Mol. Phylogenet. Evol. 9, 585–598.

Gysin, J., 1988. Animal models: primates. In: Sherman, I.W. (Ed.), Malaria: Parasite Biology, Pathogenesis, and Protection. ASM Press, pp. 419–439.

Hasegawa, M., Kishino, H., Yano, T., 1985. Dating of the human–ape splitting by a molecular clock of mitochondrial DNA. J. Mol. Evol. 22, 160–174.
Hillis, D.B., Bull, J.J., 1993. An empirical test of bootstrapping as a method for assessing confidence in phylogenetic analysis. Syst. Biol. 182–192.
Huelsenbeck, J.P., Ronquist, F., 2001. MRBAYES: Bayesian inference of phylogenetic trees. Bioinformatics 17, 754–755.
Hughes, A.L., Yeager, M., 1998. Natural selection at major histocompatibility complex loci of vertebrates. Annu. Rev. Genet. 32, 415–435.
Humphrey, W., Dalke, A., Schulten, K., 1996. VMD: visual molecular dynamics. J. Mol. Graph. 14 (33–38), 27–38.
Jobb, G., Von Haeseler, A., Strimmer, K., 2004. TREEFINDER: a powerful graphical analysis environment for molecular phylogenetics. BMC Evol. Biol. 4, 18.
Jones, D.T., Taylor, W.R., Thornton, J.M., 1992. The rapid generation of mutation data matrices from protein sequences. Comput. Appl. Biosci. 8, 275–282.
Kelley, J., Walter, L., Trowsdale, J., 2005. Comparative genomics of major histocompatibility complexes. Immunogenetics 56, 683–695.
Kimura, M., 1980. A simple method for estimating evolutionary rates of base substitutions through comparative studies of nucleotide sequences. J. Mol. Evol. 16, 111–120.
Klein, J., 1987. Origin of major histocompatibility complex polymorphism: the trans-species hypothesis. Hum. Immunol. 19, 155–162.
Klein, J., O'huigin, C., Figueroa, F., Mayer, W.E., Klein, D., 1993a. Different modes of MHC evolution in primates. Mol. Biol. Evol. 10, 48–59.
Klein, J., Satta, Y., O'huigin, C., Takahata, N., 1993b. The molecular descent of the major histocompatibility complex. Annu. Rev. Immunol. 11, 269–295.
Klein, J., Sato, A., Nagl, S., O'huigín, C., 1998. Molecular trans-species polymorphism. Annu. Rev. Ecol. Syst. 29, 1–21.
Kosakovsky-Pond, S.K., Muse, S.V., 2005. Site-to-site variation of synonymous substitution rates. Mol. Biol. Evol. 22, 2375–2385.
Kosakovsky-Pond, S.L., Frost, S.D., 2005a. Datamonkey: rapid detection of selective pressure on individual sites of codon alignments. Bioinformatics 21, 2531–2533.
Kosakovsky-Pond, S.L., Frost, S.D., 2005b. Not so different after all: a comparison of methods for detecting amino acid sites under selection. Mol. Biol. Evol. 22, 1208–1222.
Kosakovsky-Pond, S.L., Frost, S.D., Muse, S.V., 2005. HyPhy: hypothesis testing using phylogenies. Bioinformatics 21, 676–679.
Kriener, K., O'huigin, C., Klein, J., 2000a. Alu elements support independent origin of prosimian, platyrrhine, and catarrhine Mhc-DRB genes. Genome Res. 10, 634–643.
Kriener, K., O'huigin, C., Tichy, H., Klein, J., 2000b. Convergent evolution of major histocompatibility complex molecules in humans and new world monkeys. Immunogenetics 51, 169–178.
Kriener, K., O'huigin, C., Klein, J., 2001. Independent origin of functional MHC class II genes in humans and new world monkeys. Hum. Immunol. 62, 1–14.
Lujan, R., Chapman Jr., W.L., Hanson, W.L., Dennis, V.A., 1986. *Leishmania braziliensis*: development of primary and satellite lesions in the experimentally infected owl monkey, *Aotus trivirgatus*. Exp. Parasitol. 61, 348–358.
May, J., Kremsner, P.G., Milovanovic, D., Schnittger, L., Loliger, C.C., Bienzle, U., et al., 1998. HLA-DP control of human *Schistosoma haematobium* infection. Am. J. Trop. Med. Hyg. 59, 302–306.
Nei, M., Gojobori, T., 1986. Simple methods for estimating the numbers of synonymous and nonsynonymous nucleotide substitutions. Mol. Biol. Evol. 3, 418–426.
Nicholas, K.B., Nicholas, H.B., Deerfield, D.W., 1997. Genedoc. Analysis and visualization of genetic variation. EMBNEW NEWS 4, 14.
Niño-Vasquez, J.J., Vogel, D., Rodriguez, R., Moreno, A., Patarroyo, M.E., Pluschke, G., et al., 2000. Sequence and diversity of DRB genes of *Aotus nancymaae*, a primate model for human malaria parasites. Immunogenetics 51, 219–230.
Noya, O., Gonzalez-Rico, S., Rodriguez, R., Arrechedera, H., Patarroyo, M.E., Alarcon De Noya, B., 1998. *Schistosoma mansoni* infection in owl monkeys (*Aotus nancymai*): evidence for the early elimination of adult worms. Acta Trop. 70, 257–267.
O'huigin, C., 1995. Quantifying the degree of convergence in primate Mhc-DRB genes. Immunol. Rev. 143, 123–140.
Opazo, J.C., Wildman, D.E., Prychitko, T., Johnson, R.M., Goodman, M., 2006. Phylogenetic relationships and divergence times among new world monkeys (Platyrrhini, Primates). Mol. Phylogenet. Evol. 40, 274–280.
Osada, N., Hashimoto, K., Kameoka, Y., Hirata, M., Tanuma, R., Uno, Y., et al., 2008. Large-scale analysis of *Macaca fascicularis* transcripts and inference of genetic divergence between *M. fascicularis* and *M. mulatta*. BMC Genomics 9, 90.
Otting, N., Bontrop, R.E., 1995. Evolution of the major histocompatibility complex DPA1 locus in primates. Hum. Immunol. 42, 184–187.
Pico De Coana, Y., Rodriguez, J., Guerrero, E., Barrero, C., Rodriguez, R., Mendoza, M., et al., 2003. A highly infective *Plasmodium vivax* strain adapted to *Aotus* monkeys: quantitative haematological and molecular determinations useful for *P. vivax* malaria vaccine development. Vaccine 21, 3930–3937.
Piontkivska, H., Nei, M., 2003. Birth-and-death evolution in primate MHC class I genes: divergence time estimates. Mol. Biol. Evol. 20, 601–609.
Polotsky, Y.E., Vassell, R.A., Binn, L.N., Asher, L.V., 1994. Immunohistochemical detection of cytokines in tissues of *Aotus* monkeys infected with hepatitis A virus. Ann. NY Acad. Sci. 730, 318–321.
Poon, A.F., Frost, S.D., Pond, S.L., 2009. Detecting signatures of selection from DNA sequences using Datamonkey. Methods Mol. Biol. 537, 163–183.
Posch, P.E., Araujo, H.A., Creswell, K., Praud, C., Johnson, A.H., Hurley, C.K., 1995. Microvariation creates significant functional differences in the DR3 molecules. Hum. Immunol. 42, 61–71.
Posch, P.E., Hurley, C.K., Geluk, A., Ottenhoff, T.H., 1996. The impact of DR3 microvariation on peptide binding: the combinations of specific DR beta residues critical to binding differ for different peptides. Hum. Immunol. 49, 96–105.
Robinson, J., Waller, M.J., Parham, P., De Groot, N., Bontrop, R., Kennedy, L.J., et al., 2003. IMGT/HLA and IMGT/MHC: sequence databases for the study of the major histocompatibility complex. Nucleic Acids Res. 31, 311–314.
Rodriguez, R., Moreno, A., Guzman, F., Calvo, M., Patarroyo, M.E., 1990. Studies in owl monkeys leading to the development of a synthetic vaccine against the asexual blood stages of *Plasmodium falciparum*. Am. J. Trop. Med. Hyg. 43, 339–354.
Ronquist, F., Huelsenbeck, J.P., 2003. MrBayes 3: Bayesian phylogenetic inference under mixed models. Bioinformatics 19, 1572–1574.
Rzhetsky, A., Nei, M., 1993. Theoretical foundation of the minimum-evolution method of phylogenetic inference. Mol. Biol. Evol. 10, 1073–1095.
Schwarz, R., Dayhoff, M., 1979. Matrices for detecting distant relationships. In: Dayhoff, M. (Ed.), Atlas of protein sequences. National Biomedical Research Foundation, pp. 353–358.
Shimodaira, H., Hasegawa, M., 1999. Multiple comparisons of log-likelihoods with applications to phylogenetic inference. Mol. Biol. Evol. 16, 1114–1116.
Sitnikova, T., 1996. Bootstrap method of interior-branch test for phylogenetic trees. Mol. Biol. Evol. 13, 605–611.
Slierendregt, B.L., Otting, N., Kenter, M., Bontrop, R.E., 1995. Allelic diversity at the Mhc-DP locus in rhesus macaques (*Macaca mulatta*). Immunogenetics 41, 29–37.
Steiper, M.E., Young, N.M., 2006. Primate molecular divergence dates. Mol. Phylogenet. Evol. 41, 384–394.
Stern, L.J., Brown, J.H., Jardetzky, T.S., Gorga, J.C., Urban, R.G., Strominger, J.L., et al., 1994. Crystal structure of the human class II MHC protein HLA-DR1 complexed with an influenza virus peptide. Nature 368, 215–221.
Suarez, C.F., Patarroyo, M.E., Trujillo, E., Estupiñan, M., Baquero, J.E., Parra, C., et al., 2006. Owl monkey MHC-DRB exon 2 reveals high similarity with several HLA-DRB lineages. Immunogenetics 58, 542–558.
Takahashi, K., Rooney, A.P., Nei, M., 2000. Origins and divergence times of mammalian class II MHC gene clusters. J. Hered. 91, 198–204.
Tamura, K., Kumar, S., 2002. Evolutionary distance estimation under heterogeneous substitution pattern among lineages. Mol. Biol. Evol. 19, 1727–1736.
Tamura, K., Nei, M., Kumar, S., 2004. Prospects for inferring very large phylogenies by using the neighbor-joining method. Proc. Natl Acad. Sci. USA 101, 11030–11035.
Tamura, K., Dudley, J., Nei, M., Kumar, S., 2007. MEGA4: Molecular Evolutionary Genetics Analysis (MEGA) software version 4.0. Mol. Biol. Evol. 24, 1596–1599.
Thompson, J.D., Gibson, T.J., Plewniak, F., Jeanmougin, F., Higgins, D.G., 1997. The CLUSTAL_X windows interface: flexible strategies for multiple sequence alignment aided by quality analysis tools. Nucleic Acids Res. 25, 4876–4882.
Trtkova, K., Mayer, W.E., O'huigin, C., Klein, J., 1995. Mhc-DRB genes and the origin of new world monkeys. Mol. Phylogenet. Evol. 4, 408–419.
Yuhki, N., Beck, T., Stephens, R.M., Nishigaki, Y., Newmann, K., O'brien, S.J., 2003. Comparative genome organization of human, murine, and feline MHC class II region. Genome Res. 13, 1169–1179.